

SIMS analysis of coated Nb samples

SQMS Summer Internship Report

Author : Francesco Cioni *

Supervisors : Akshay Murthy †

October 2022



**SUPERCONDUCTING QUANTUM
MATERIALS & SYSTEMS CENTER**

¹University of Pisa, Department of Physics "E. Fermi"

²Superconducting Quantum Materials and Systems Center, Fermi National Accelerator Laboratory

Abstract

The project focuses on characterizing the growth of oxides on top of Niobium samples, and the effects of adding an additional layer of a different superconductor on top of them.

Contents

1	Introduction	1
1.1	The Standard Tunneling Model	1
1.2	Probing individual TLSs	2
1.3	Dielectric losses in qubits and SRF cavities	3
1.4	Secondary Ion Mass Spectrometry	5
1.5	SIMS analysis of Niobium samples	5
2	Results	6
2.1	Main result of the analysis	6
2.2	Ti on Nb system	8
2.2.1	Time study	8
2.2.2	Heating study	12
2.3	TiN on Nb system	15
2.3.1	Time study	15
2.3.2	Heating study	16
3	Conclusions	17

1 Introduction

In recent years, superconducting materials have been used extensively for both fundamental and technological research. Superconducting radio-frequency (SRF) cavities with photon lifetime of tens of seconds and quality factor $Q > 10^{10} - 10^{11}$ are currently used in particle accelerators. At the same time, superconducting thin films are used in the fabrication of transmon qubits, where coherence times up to hundreds of μs have been achieved.

To increase further the performance of such devices, one needs to eliminate the various sources of losses in the system. At present, one of the major problems that the quantum community is facing is mitigating the effects of two-level systems (TLS) usually residing at dielectric/metal interfaces.

The origin of such TLSs may be multiple, but it is clear that tunneling systems in amorphous materials can lead to such losses. These are formed by defects that can be in two different configurations connected by a finite tunneling amplitude (Fig.1). In the next section we will outline the theoretical framework that has been developed to model such systems.

1.1 The Standard Tunneling Model

Given the amorphous nature of the host material, the parameters of such systems span a wide range of values, and one needs to assume a specific form of the distribution of such parameters. The theory that is usually used to describe such ensembles is called the Standard Tunneling Model (STM) [1]. This theory only needs two parameters ε and Δ_0 that we are now going to define, the distribution of such parameters over the ensemble of TLS and the TLS response to external perturbations.

The Hamiltonian for such a system is:

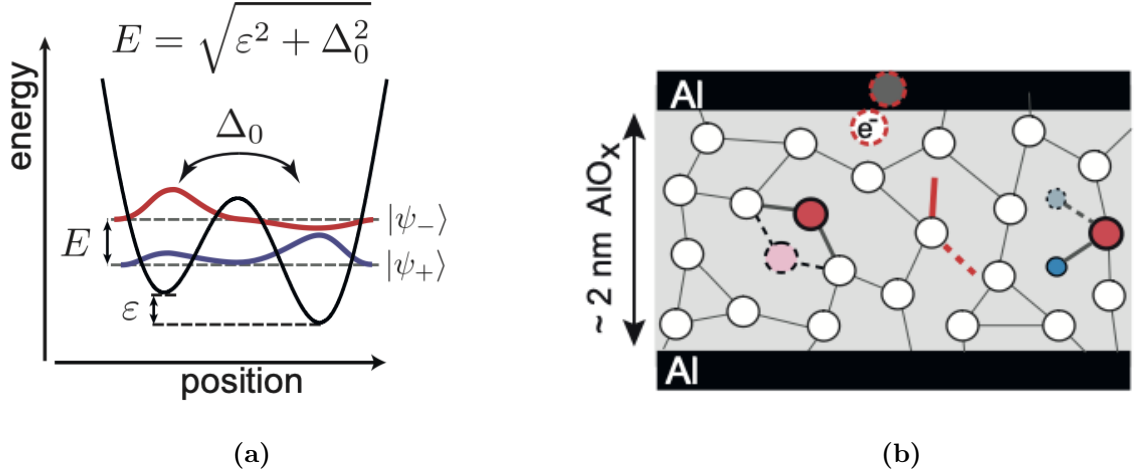


Figure 1: (a) Energy diagram and (b) physical origins of two-level systems

$$H_{TLS} = \frac{1}{2} \begin{pmatrix} \varepsilon & \Delta_0 \\ \Delta_0 & -\varepsilon \end{pmatrix} = \frac{1}{2} \varepsilon \sigma_z^{(p)} + \frac{1}{2} \Delta_0 \sigma_x^{(p)} \quad (1)$$

where the upper letter (p) indicates that these are Pauli matrices in the position basis $\{|L\rangle, |R\rangle\}$. For simplicity, we are imagining a TLS formed by an atom that can be in two different spatial configurations. For other types of TLSs, the position variable can be substituted with the relevant configuration variable. The graphical interpretation of ε and Δ_0 can be seen in (Fig 1a). Due to the finite tunneling amplitude Δ_0 , the states in the left and right well hybridise, forming the two eigenstates:

$$|+\rangle = \sin(\theta/2) |L\rangle + \cos(\theta/2) |R\rangle \quad (2)$$

$$|-\rangle = \cos(\theta/2) |L\rangle - \sin(\theta/2) |R\rangle \quad (3)$$

where $\tan \theta = \Delta_0/\varepsilon$. The energy splitting between the two is:

$$E = E_+ - E_- = \sqrt{\varepsilon^2 + \Delta_0^2} \quad (4)$$

To proceed, one needs to choose the relevant pair of variables and specify the distribution of such variables. Different distributions lead to different kinds of noise, and it was demonstrated that the typically observed noise spectra can be described using such ensembles [2].

1.2 Probing individual TLSs

In the last decade, it also became possible to use qubits strongly coupled to individual TLSs residing in the Josephson Junction's oxide layer as a probe to measure the physical properties of the TLS itself [3] and to observe TLS-TLS interactions [4]. These measurements rely on the possibility to tune both the frequency of the phase qubit and the ε parameter of the TLS. This is typically done by bending the qubit chip with a piezo actuator to create a strain field \mathbf{S} at the TLS position (inset Fig 2). The field couples with the TLS in such a way that:

$$\delta\varepsilon = 2\boldsymbol{\gamma} \cdot \mathbf{S} \quad (5)$$

where $\boldsymbol{\gamma}$ is the analogous of the dipole moment \mathbf{p} in the case of electric coupling.

Electric coupling would give a similar contribution to $\delta\varepsilon$. Anyway that is not used for frequency tuning because it would be more difficult to prevent the qubit from coupling directly to the field.

Whenever a TLS and a qubit come into resonance, exchange of energy between the two systems become possible, and this results in a swapping of the states of the two. Wide ranges of frequency are spanned for both TLS and qubit, and a change in the qubit's excited state population is observed whenever its frequency is equal to the one of a TLS. In this way one can map the energies of all the TLSs that couple to the qubit and observe their dependence on the applied strain field (Fig 2).

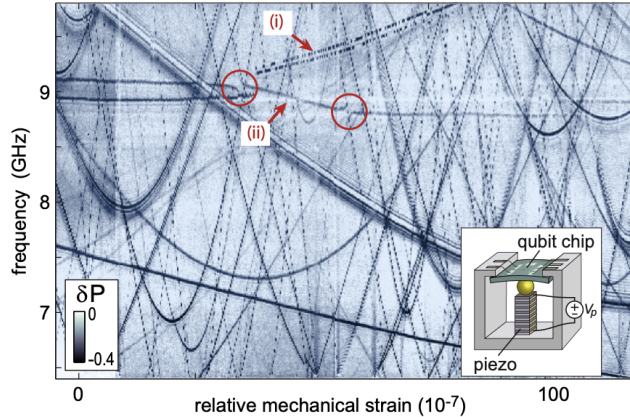


Figure 2: Variation δP (color-coded) of the qubit population as a function of both qubit's and TLS' frequency. The darker traces correspond to the energy of each TLS. The hyperbolic dependence on ε predicted by (4) is clearly seen. TLS-TLS interactions cause (i) telegraphic switching, (ii) non-hyperbolic traces and (circle) avoided level crossings. [1]

These experiments allowed to measure properties like the TLS relaxation time T_1 or the coupling factor γ (found to be $\sim 0.1 - 1$ eV). The relaxation times were found to vary from approximately 10 to 1000 ns depending on the coupling strength to the qubit [5].

1.3 Dielectric losses in qubits and SRF cavities

Dielectric losses arise from the coupling of the TLSs to the external electric field via their dipole moment \mathbf{p} . The relevant parameter used to characterize such losses is the loss tangent $\tan \delta \equiv \text{Im}\{\epsilon\}/\text{Re}\{\epsilon\}$ where ϵ is the dielectric constant of the insulator. To obtain longer coherence times, smaller loss tangents $\tan \delta \ll 10^{-5}$ are required.

In 2005, [6] measured the loss tangent of an LC oscillator where a 300nm thick CVD SiO_2 capacitor was used. The results are shown in (Fig. 3a)

The losses are inversely proportional to the driving amplitude and saturate at $\delta \sim 10^{-3}$. A similar value was measured in the case of an AlO_x capacitor. Also, the losses are seen to be a lot smaller for CVD Silicon Nitride. This reflects in a longer coherence time for phase qubits built using SiN as the dielectric (Fig. 3b).

In the paper, they suggest that the dominant source of losses in CVD SiO_2 and AlO_x are OH defects. This means that a fundamental role in qubit's performance is played by the quality of the materials used, and hence by the fabrication method.

In recent years, the study of SRF cavities has become relevant also for the quantum computing community. This is due to the advent of the Transmon qubit, which needs such resonators to work.

The cavity working regime required by such architectures is different from the one used in typical high energy physics experiments. As a matter of fact the low temperature and low power (few photons) limit is needed.

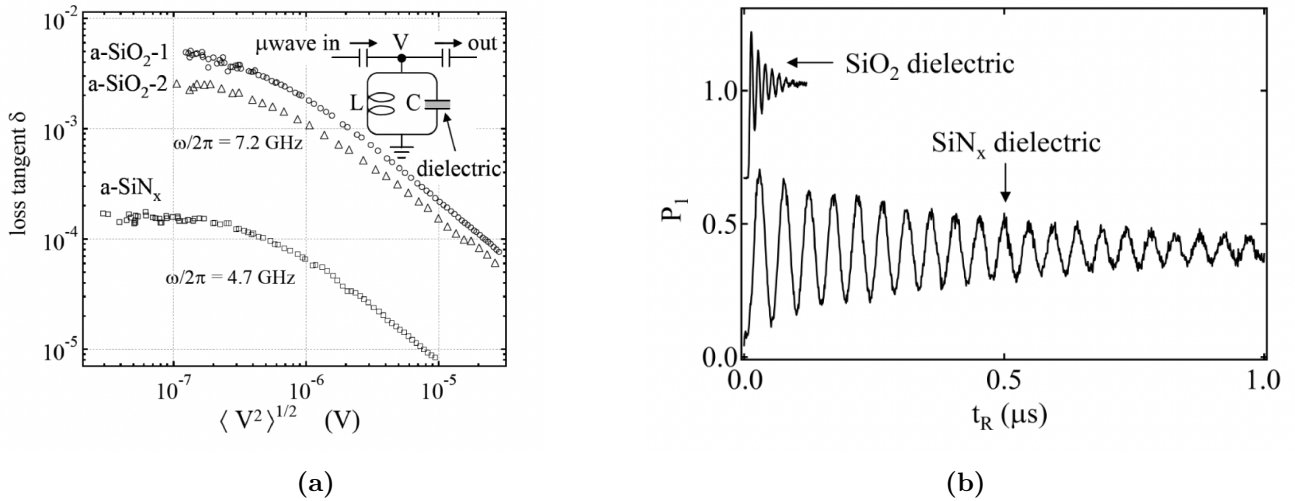


Figure 3: (a) Loss tangents measurements as a function of the driving amplitude for different samples. (b) Rabi oscillations for two phase qubits with different dielectrics used in the fabrication. [6]

Measurements of the Q factor of some cavities as a function of the temperature [7] are shown in Fig. 4a.

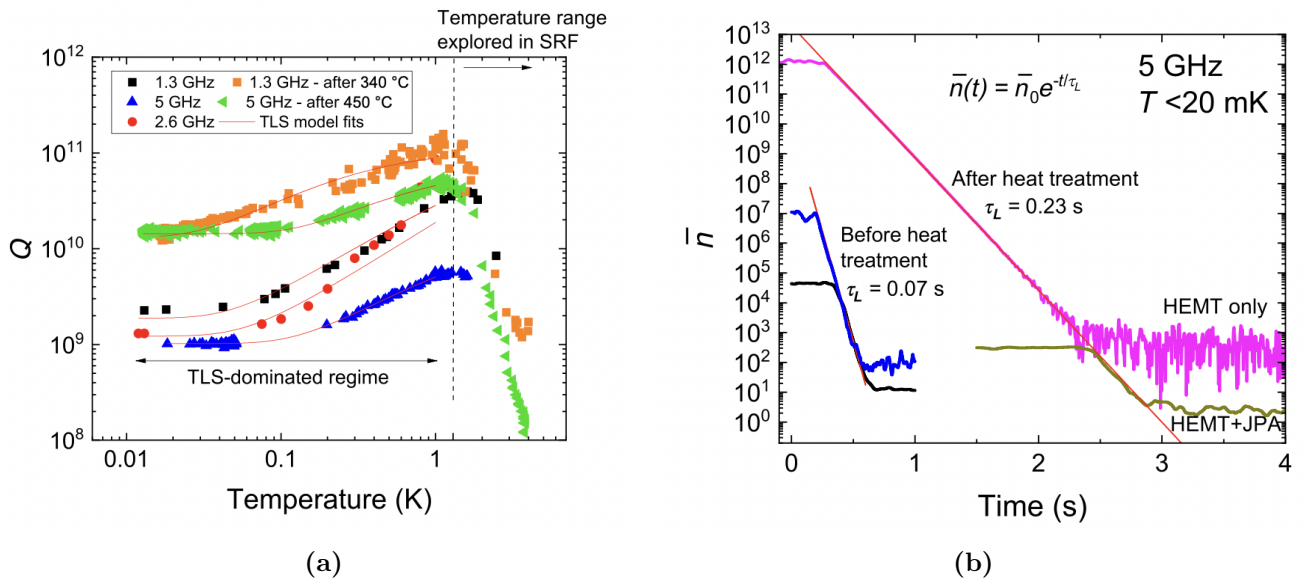


Figure 4: (a) Cavity quality factor Q of the 1.3, 2.6 and 5 GHz cavities as a function of the temperature. Data from the same cavities after heat treatment are also shown. (b) Average photon population decay in the 5 GHz cavities before and after heat treatment at 450°C. [7]

For every cavity a decrease in performances below 1K is clearly seen. Since the typical energy splitting of the TLSs is \sim GHz, above 1K the Boltzmann factor $\exp(-E/kT) \sim 1$ and the TLSs are saturated. This results in a decrease in dielectric losses at high temperature.

How can one reduce such losses? In Fig. 4a are shown the data from two cavities, before and after being heated in vacuum at or above 350°C. The heat treatment result in an improvement of an order of magnitude in the performance.

The reduction in dielectric losses is associated with the removal of the amorphous oxide layer (Nb₂O₅) growth on top of the Niobium used to build the cavity. This was confirmed by a TOF-SIMS study of the cavity (in Chapter 2 we will talk a bit more in depth about this method). Such improvements directly reflect in a much bigger photon lifetime (see

Fig. 4b).

1.4 Secondary Ion Mass Spectrometry

Secondary Ion Mass Spectrometry (SIMS) is a useful method to obtain information about the oxides that grow on top of superconductors. Out of all the things that SIMS can do, we are mostly interested in its "dynamic" mode, which allows to measure the chemical composition of a sample as a function of the depth. This is done using two ion guns. The *sputter gun* is a high intensity beam that erodes the sample to allow depth profiling. The *primary gun* on the other hand is a 30keV ion gun that allows the ionization of a fraction of the atom in the material, which are then captured by an electric field that takes them in a mass spectrometer where they are identified.

The ionization process is very complicated and quantitative results are difficult to obtain using SIMS. The ionization rate for example can depend on the ion beam current, the pressure in the chamber, the atomic species and other factors. In addition, the counts of some molecules may be affected by the decomposition of higher stoichiometry ones (for example Nb_2O_5 into NbO or NbO_2) and also by the environment they are in. An example of such misreading can be seen in Fig. 6. These data are taken from Niobium coated with Aluminum and Titanium respectively, and represent the depth profile (from left to right) of the samples. In Fig. 5a the Nb counts are higher in the Al region than they are in the bulk of the Nb sample, while in Fig. 5b the Nb_2O_5 counts are higher at the Ti-vacuum interface than they are at the Ti-Nb interface. This suggests that care must be taken before interpreting quantitatively a SIMS result.

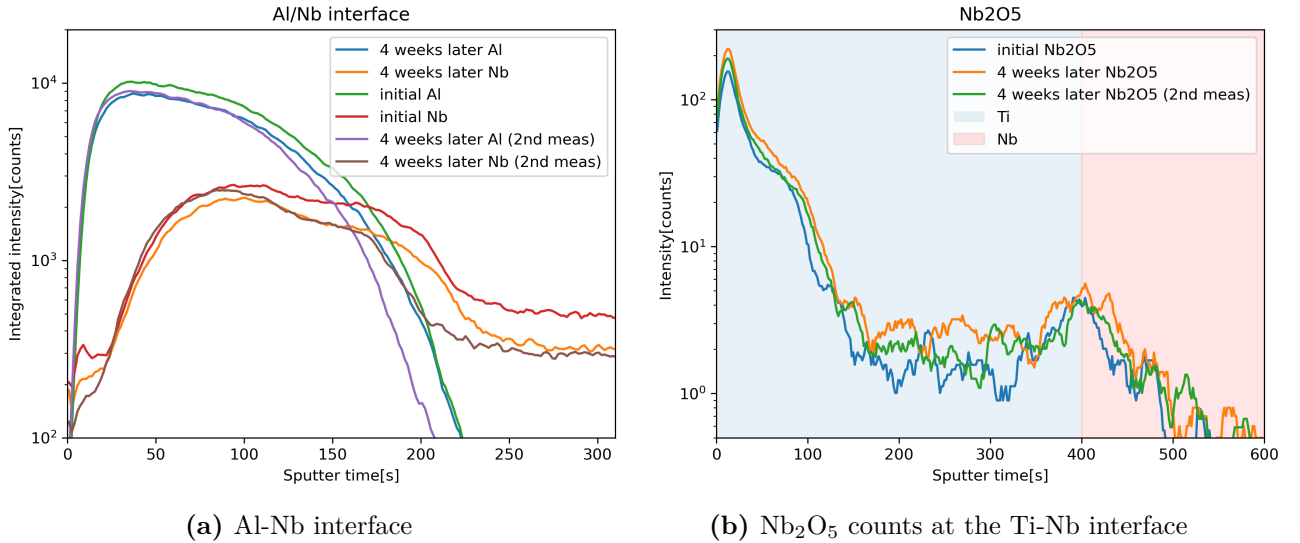


Figure 5

1.5 SIMS analysis of Niobium samples

SIMS analysis of Nb samples have been performed in the past, observing the effects of various heating cycles or chemical treatments [8]. It has been observed that a NbO_x layer of approximately 5nm forms when the sample is put in contact with air. This layer disappears after being heated above 350°C for at least 2 hours. This decrease is accompanied by an increase in NbC counts at the surface (Fig. 6a). Other effects include the reduction in the Hydrogen bulk concentration (Fig. 6b).

In this project, SIMS measurements have been made on Niobium samples coated with an additional layer of a different metal to check if the coating can prevent the formation of

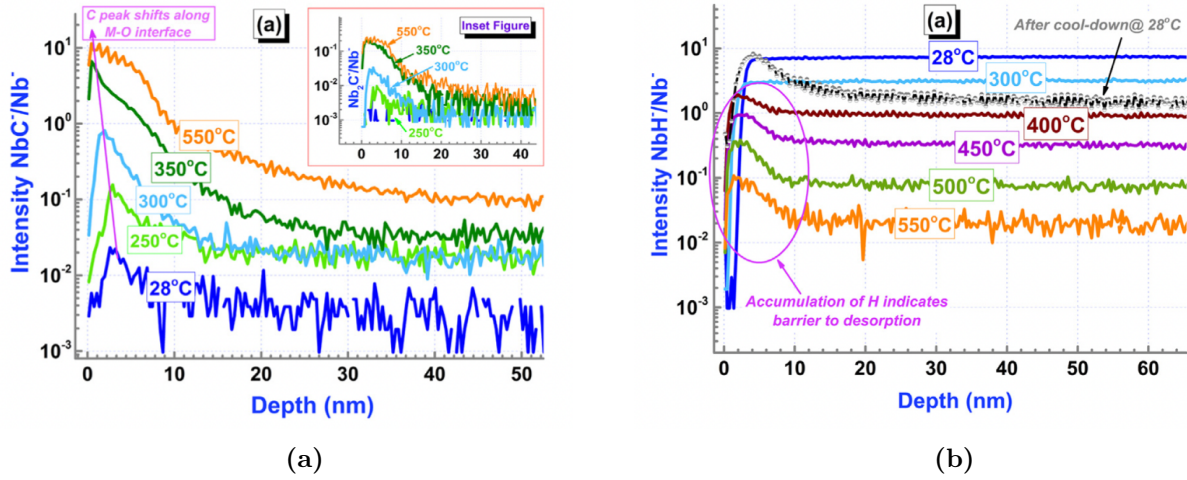


Figure 6: (a)NbC and (b)NbH counts for various heat treatments. Data taken from [8]

oxides. A schematic of the structure is shown in Fig. 7. The results of the measurements are shown in the next section.

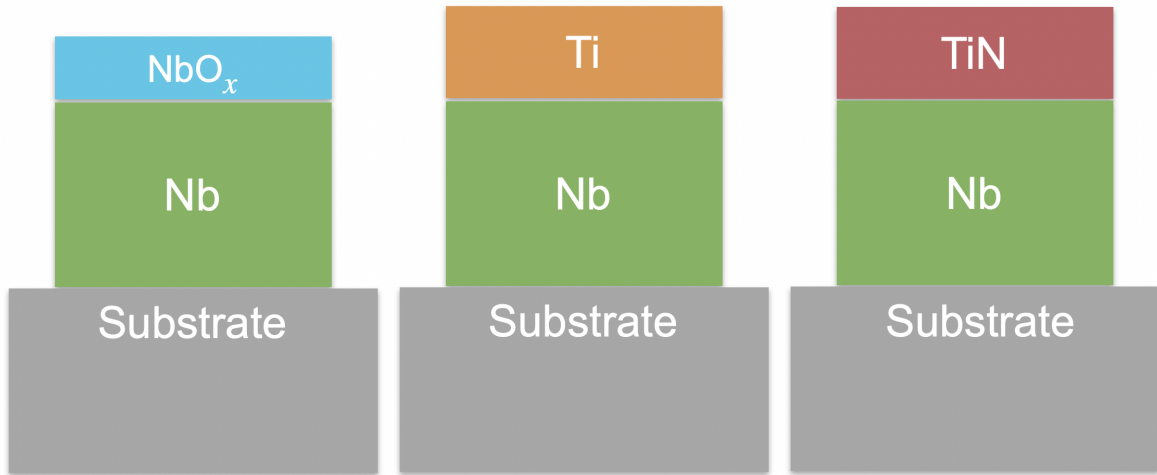


Figure 7: Schematic of the structure of the samples

2 Results

2.1 Main result of the analysis

The primary goal of this fabrication technique is to prevent the formation of Nb-oxides on the Nb surface. We can readily see that such result is obtained. In Figs. 8, 9 and 10 are shown the Nb_2O_5 counts for, respectively: a reference Nb sample, a Ti on Nb sample and a TiN on Nb sample. The oxide counts at the Nb surface are reduced by more than three orders of magnitude.

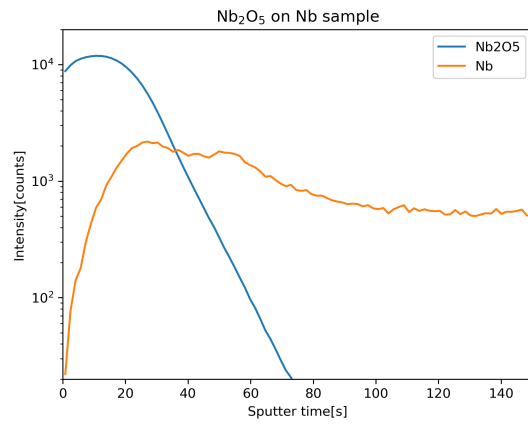


Figure 8: Nb_2O_5 counts on reference Nb sample

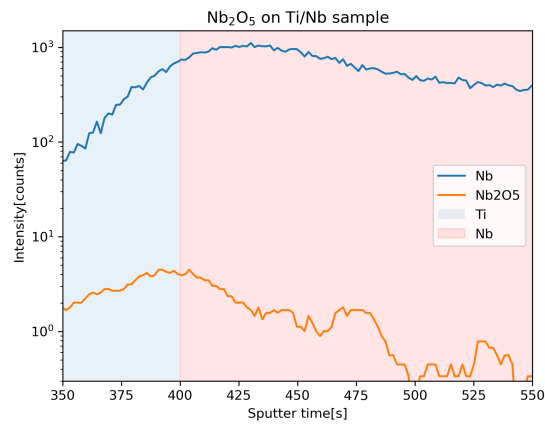


Figure 9: Nb_2O_5 counts on Ti/Nb sample

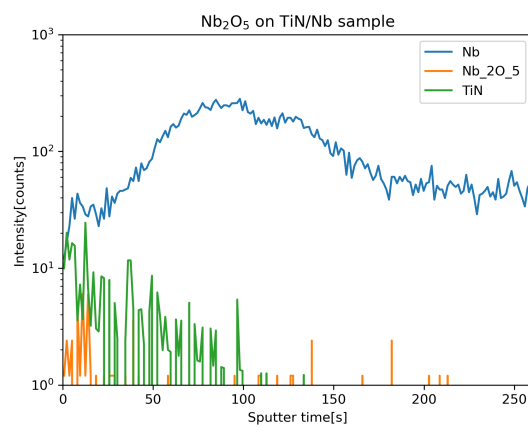


Figure 10: Nb_2O_5 counts on TiN/Nb sample

In the next sections, time studies and heating studies on the two investigated systems are presented.

2.2 Ti on Nb system

2.2.1 Time study

SIMS measurements of a Ti/Nb/Si sample were taken at three different times: (A) right after the deposition, (B) 4 weeks later and (C) 7 weeks later. For the B and C samples, two independent measurements were made at different positions to account for possible impurities present in small regions of the samples. The results from C did not show any difference with the one from B and so in what follows they are not shown for clarity.

The Ti and Nb counts at the Ti/Nb interface are shown in Fig. 11. A distinct separation of the two layer is observed. For example, this can be confronted with the Al/Nb interface in Fig. 5a which is an example of bad separation. The actual width of the interface is difficult to estimate. This is because the sputtering rate (i.e. the rate at which the surface layer is removed) depends for example on the composition of the layer and the intensity of the ion gun. Estimates are possible by measuring the width of a known layer with other methods, and then using this as a reference standard.

Anyway the distinct separation is a good feature of the Ti coating, since we expect the properties of the bulk Niobium to be preserved. Measuring the superconducting properties of these samples could be an interesting analysis. Unfortunately this was not possible due to some problems with the measuring devices.

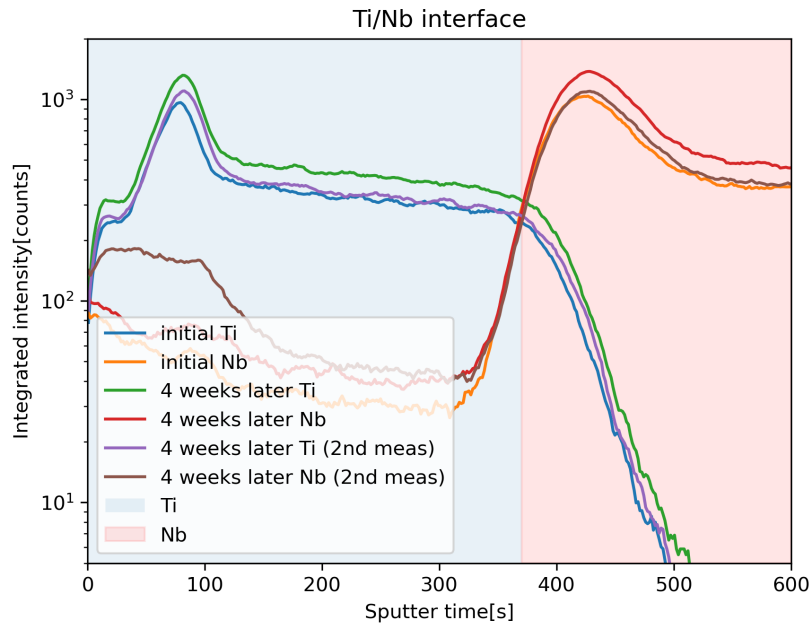


Figure 11: Titanium and Niobium counts at the Ti/Nb interface. Distinct separation of the two layers is observed.

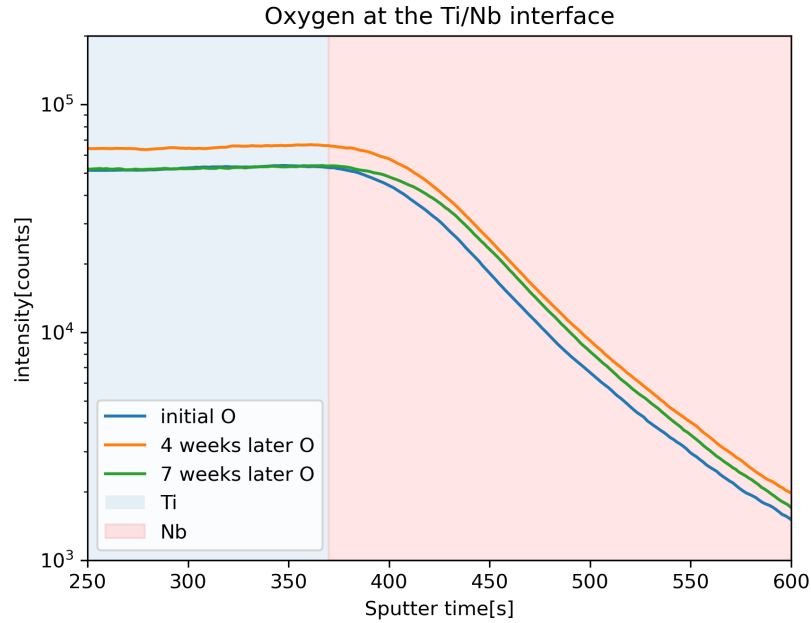


Figure 12: Oxygen counts at the Ti/Nb interface. No Oxygen diffusion over time into the Niobium layer is observed

In Fig. 12 are shown the Oxygen counts at the Ti/Nb interface. Due to the oxidization of the materials, the intensity is very high in the Ti region and starts to decay entering in the Nb bulk. Since, as explained in Section 1.3, the presence of O might be associated with TLS losses, we want the bulk Niobium to be as much as possible isolated from the Oxygen. For this reason, another good feature of this coating is that the O signal is stable during the 7 weeks and does not show diffusion into the Niobium.

As mentioned in Section 2.1, the biggest hope of this fabrication method is that by coating the Nb film right after the deposition (before being put in contact with air) we will prevent the formation of Niobium oxides. The counts of such oxides at the Ti/Nb interface are shown in Figs. 13, 14, 15. The Nb_2O_5 integrated signal is also shown in Fig. 16.

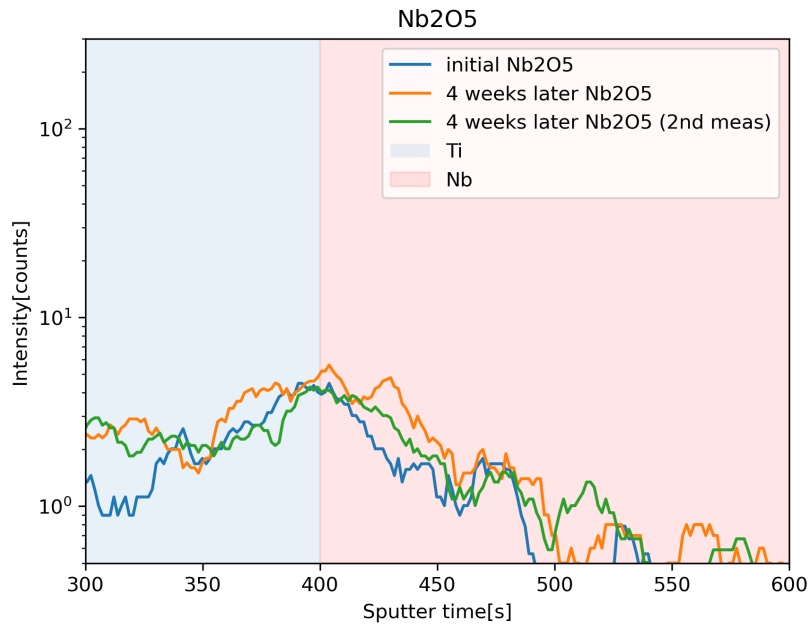


Figure 13: Nb₂O₅ counts at the Ti/Nb interface

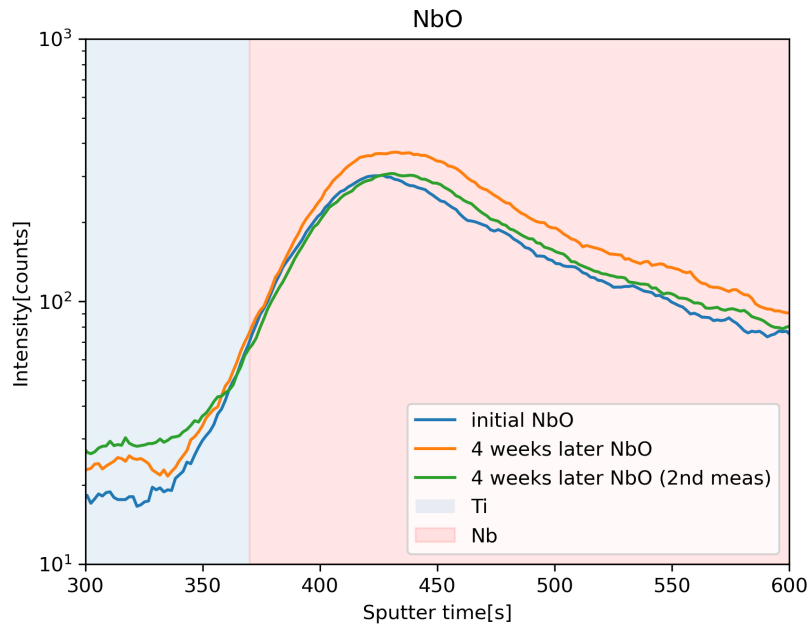


Figure 14: NbO counts at the Ti/Nb interface

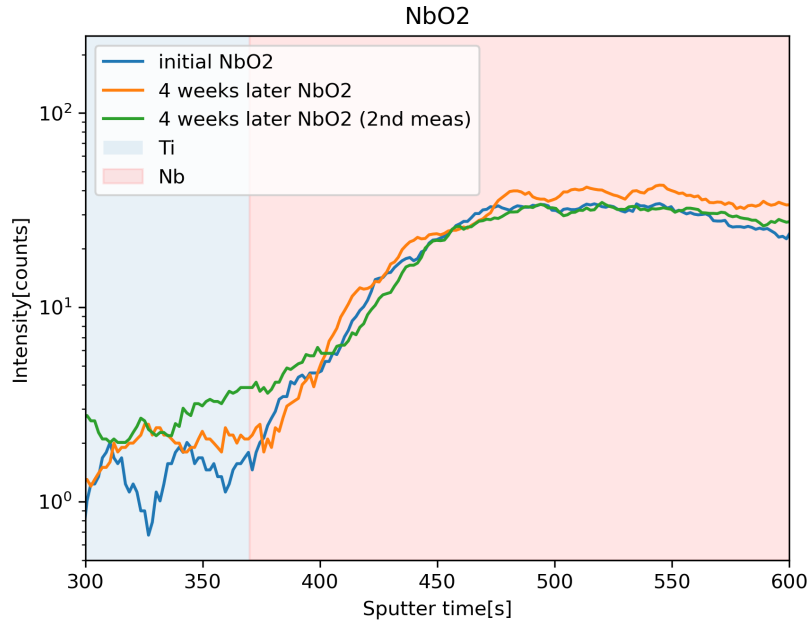


Figure 15: NbO₂ counts at the Ti/Nb interface

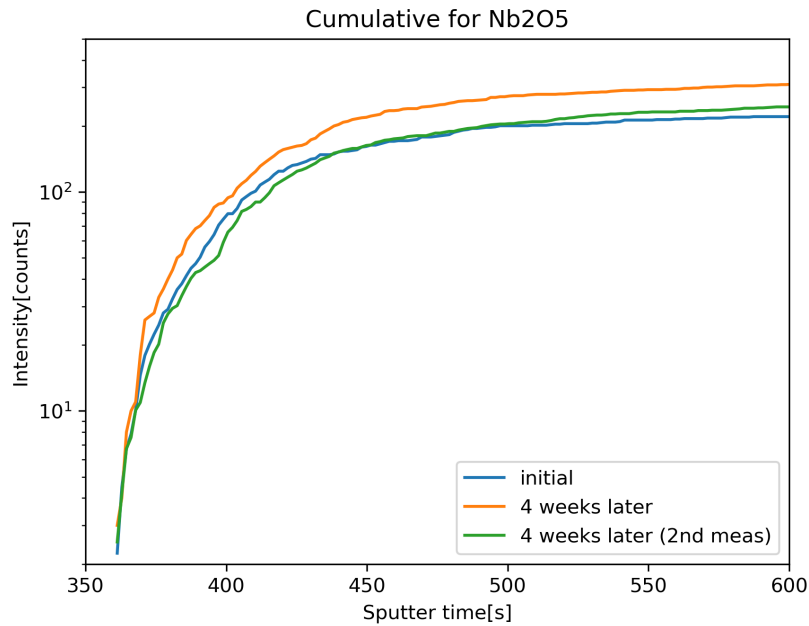


Figure 16: Nb₂O₅ integrated signal as a function of the sputtering time

These Figures show that no NbO_x growth is observed over the 7 weeks, confirming the effectiveness of the method over time.

As suggested by Fig. 12, a big amount of Oxygen is still present at the very surface of the sample. This is due to the oxidization of the Ti layer, and the formation of TiO₂ on top of it.

The TiO₂ will introduce losses in the system just like the NbO_x. Anyway, further measurements are needed to check if the combined effect of the additional Ti/Nb interface and the oxide layer make the performance worse with respect to pure Niobium. In any case, this method might provide a way to trade a given oxide layer for a better one.

2.2.2 Heating study

A different sample fabricated with the same method was used to test the effects of heating cycles. Six measurements in total were made: (A) two as a reference before any heating, (B) two after 2.5 hours at 400°C and (C) two after 2 hours at 600°C. The pressure in the chamber during the heating was around 1E-8 torr. For clarity only one measurement for each treatment is shown since no differences were seen in any pair.

The effects of the heating cycles on the Ti/Nb interface are shown in Fig. 17. The distinct separation at the interface already observed is not affected by the heating. No change is observed after the 400C treatment. On the other hand, after the 600C treatment a shift of the interface position is seen as well as a change in the shape of the Ti signal.

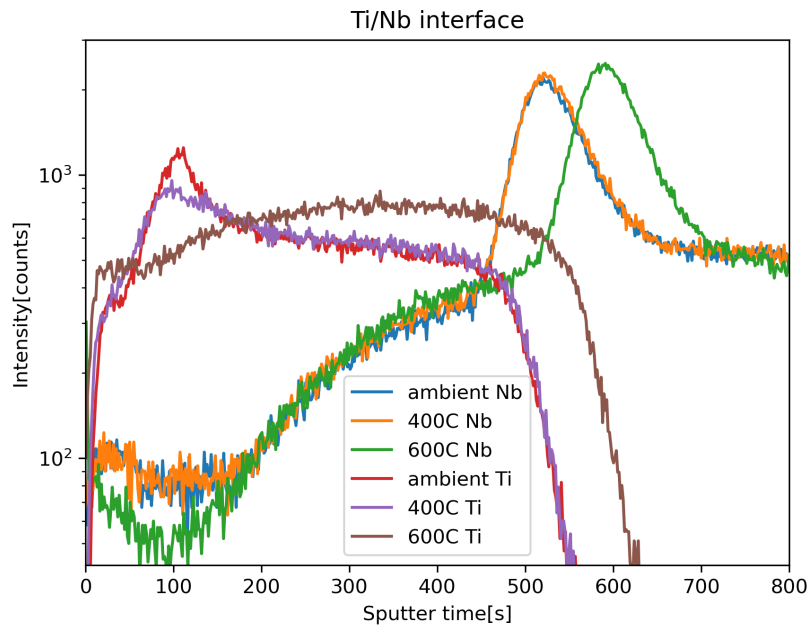


Figure 17: Titanium and Niobium counts at the Ti/Nb interface.

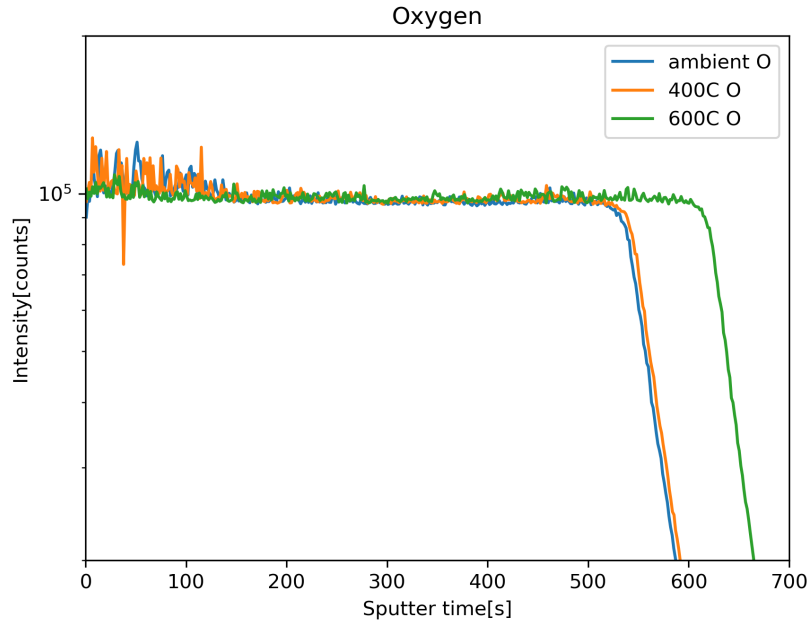


Figure 18: Oxygen counts at the Ti/Nb interface.

After the 600°C treatment, a similar shift is observed in the Oxygen signal at the Ti/Nb interface (Fig. 18). This may be due to diffusion of Oxygen into the bulk Niobium. Actually, it's not easy to confirm this assertion. Figs. 19 and 20 show the Carbon and TiO₂ counts at the surface of the sample, respectively. What is clearly seen after the 600°C treatment is an increase in Carbon and a reduction in oxide counts. This suggests that a fraction of the TiO₂ has absorbed Carbon forming a TiC layer on top of the sample. An analogous effect was observed in the case of a pure Nb sample, with the reduction of NbO_x in favor of NbC [8]. The formation of a layer with different chemical composition can also explain the change in the shape of the Ti signal seen in Fig. 17. In principle the observed shifts may be due to a smaller sputtering rate of the TiC with respect to the TiO₂ one. This fact does not allow to conclude that there is Oxygen diffusion into Niobium.

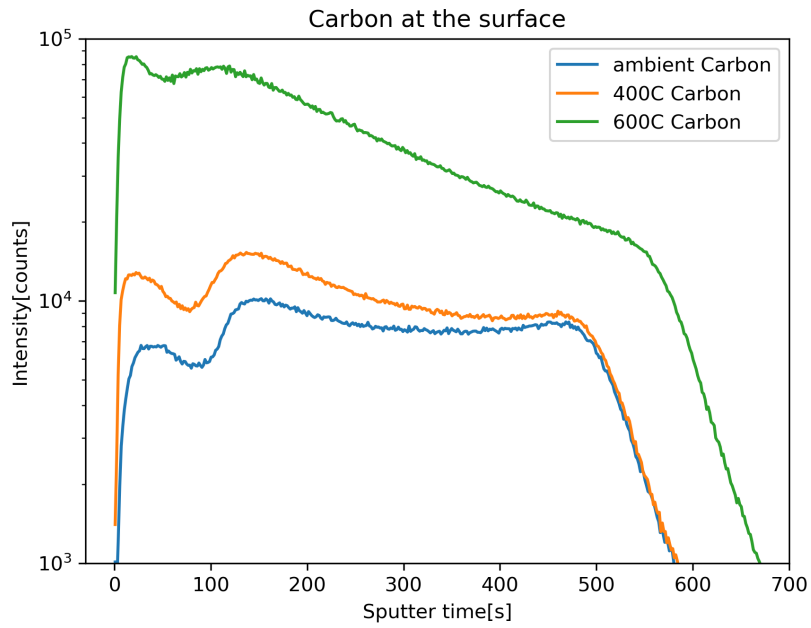


Figure 19: Carbon counts at the surface of the Ti/Nb sample.

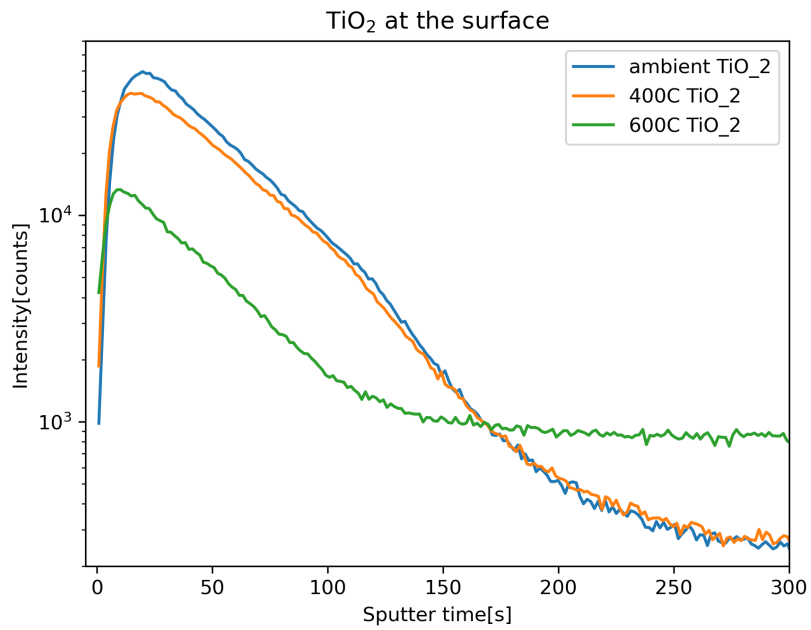


Figure 20: TiO₂ counts at the surface of the Ti/Nb sample.

Finally, a progressive reduction of Hydrogen counts with increasing temperature is observed (Fig. 21) while no clear changes were observed in the Nb₂O₅ counts (Fig. 22).

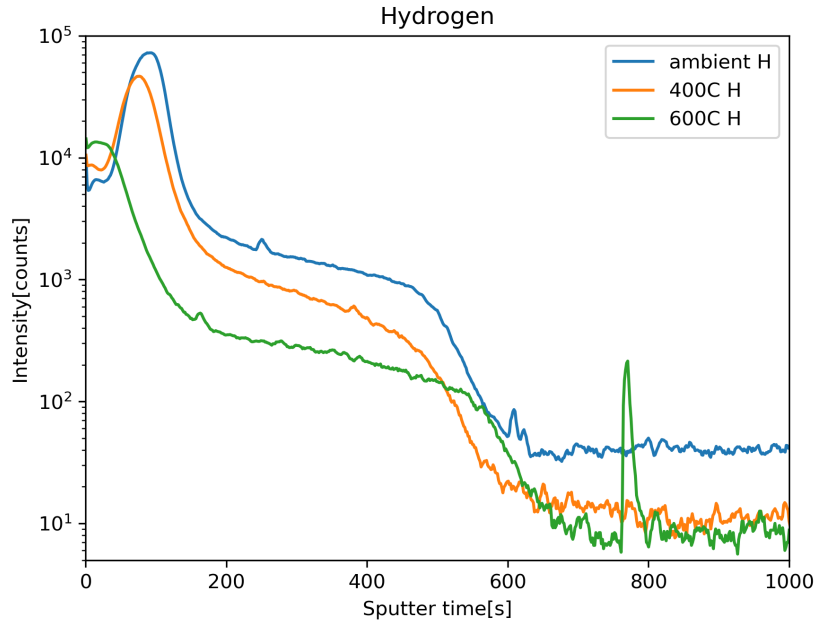


Figure 21: Hydrogen counts in the Ti/Nb sample.

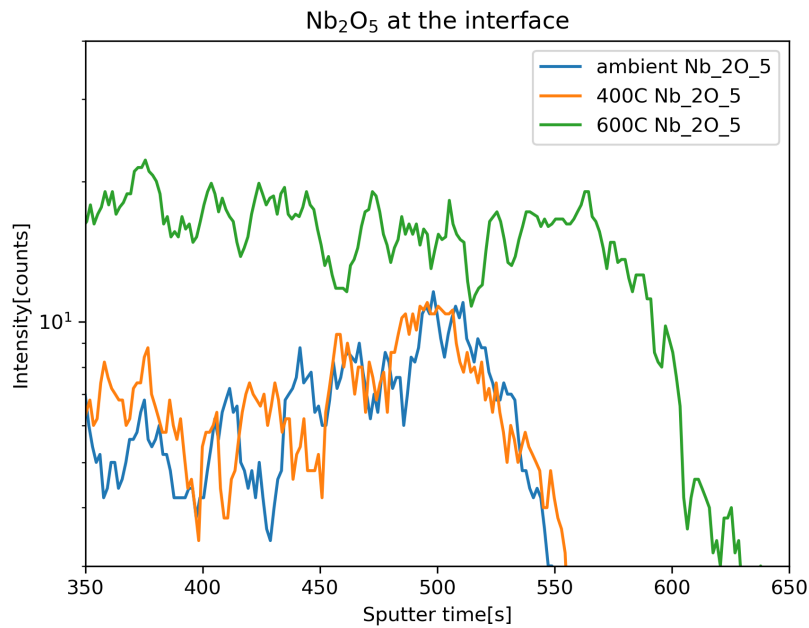


Figure 22: Nb_2O_5 counts at the Ti/Nb interface.

2.3 TiN on Nb system

2.3.1 Time study

The same kind of analysis were made on a TiN/Nb/Sapphire sample.

Let's first start with the time study. In Fig. 23 the composition of the outer surface of the TiN/Nb sample is shown. An increase in TiO_2 counts during the first 4 weeks is observed. In the same period of time, no shift of the Nb signal is observed. This observation, combined with the fact that the amount of Ti in the sample is fixed, suggests that Oxygen

is replacing a fraction of the Nitrogen in the TiN layer, forming TiO_2 . In Fig. 24 are shown the Oxygen counts in the TiN/Nb sample. Minimal diffusion into the Nb is observed over the first 4 weeks.

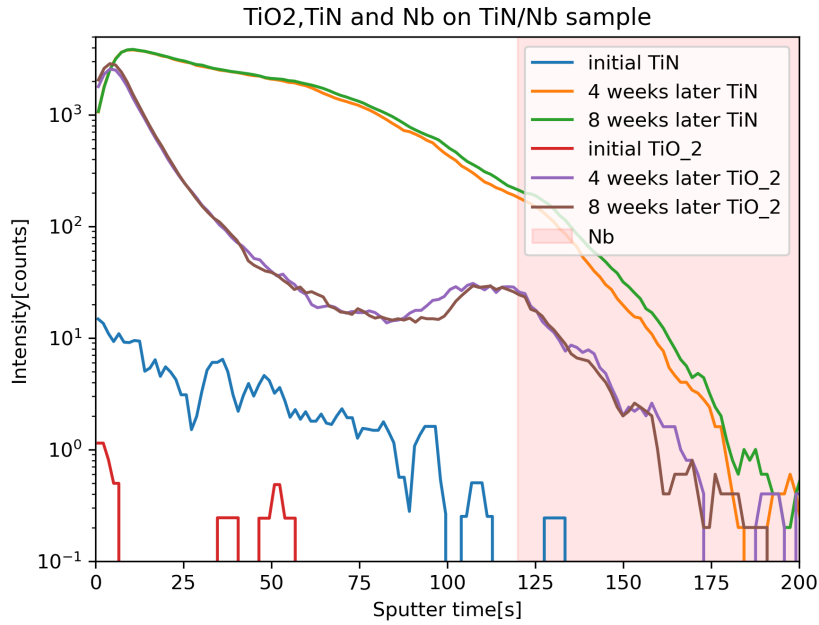


Figure 23: Increase of TiO_2 over time on TiN/Nb sample

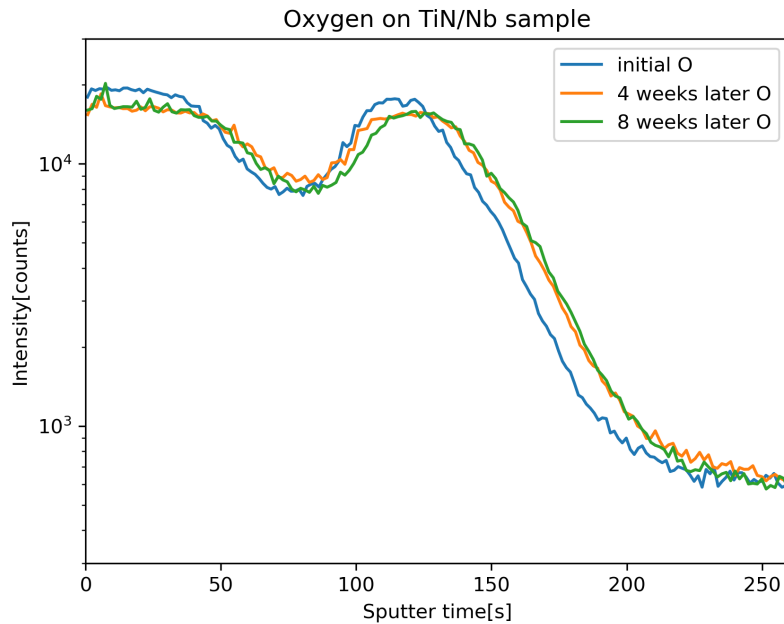


Figure 24: Sign of Oxygen diffusion at the TiN/Nb interface.

2.3.2 Heating study

Heating studies on TiN/Nb sample did not show major changes after heating cycles. In Fig. 25 are shown the TiN counts at the surface. Minimal diffusion of TiN into Nb is observed with increasing temperature. Anyway, the overall structure of the interface does not seem to be affected by the heating. In Fig. 26 the oxygen counts across the TiN layer

are shown. A small decrease is observed in the vicinity of the TiN/Nb interface after the 600C treatment. Once again, no major structural change is observed.

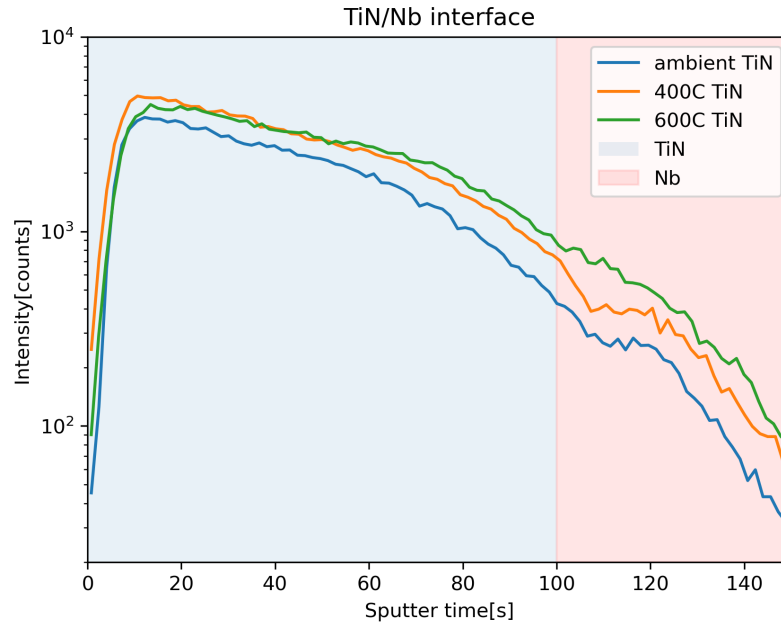


Figure 25: Minimal diffusion of the TiN layer into the Nb with increasing temperature

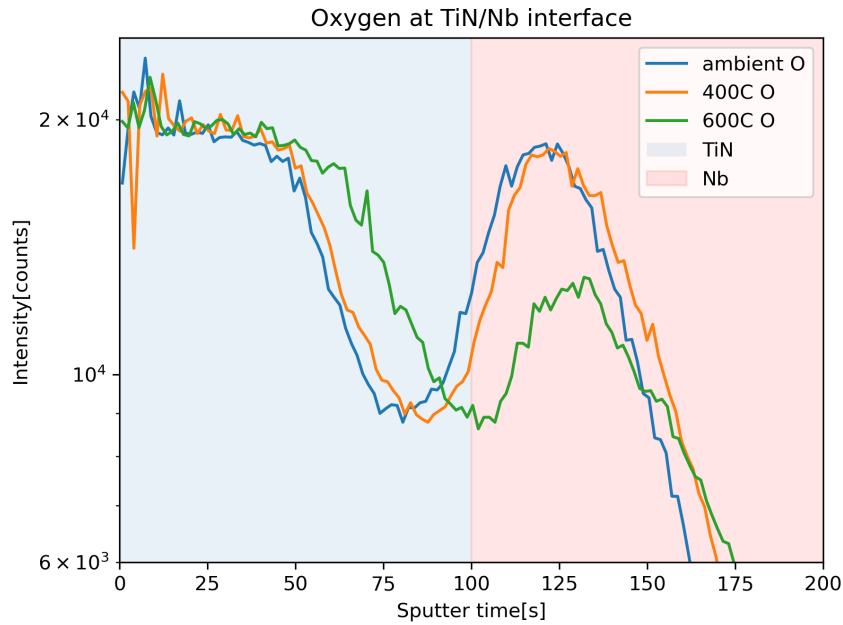


Figure 26: Small decrease of Oxygen counts at the TiN/Nb interface after 600C

3 Conclusions

In conclusion, time studies and heating studies using SIMS were made on both Ti/Nb/Si and TiN/Nb/Sapphire samples. The additional metallic layer on top of the Nb film is found to be very effective in preventing the formation of Nb-oxides. The Nb_2O_5 observed

counts are more than three orders of magnitude lower than the ones from a reference Nb sample.

The time studies indicate that this method is still effective after 7-8 weeks. A very good stability of the metal/Nb interface separation is observed in both sample. In the case of TiN on Nb, a conversion of TiN into TiO_2 is observed during the first 4 weeks. Oxygen diffusion into Nb is anyway very small in both samples.

The heating study on the Ti/Nb sample does not show major changes after the 400C treatment. After 600C, a shift in the position of the Ti/Nb interface is observed. The origin of such shift is not clear. Given that the Carbon counts at the interface increase by an order of magnitude after 600C, a possibility is that TiO_2 incorporates Carbon forming TiC. TiC can have a different sputtering rate with respect to the oxide and this may explain the shift in the interface. Finally, a reduction in Hydrogen counts are observed with increasing temperature.

As for the TiN/Nb sample, even the 600C treatment does not change significantly the structure of the sample. The TiN/Nb interface is very stable and only a minimal diffusion of TiN into Nb is observed with increasing temperature. Finally, after 600C a small decrease in Oxygen counts at the Nb surface is observed.

References

- [1] C. Muller et al. "Towards understanding two-level-systems in amorphous solids - Insights from quantum devices". In: *Rep. Prog. Phys.* 82.124501 (2019).
- [2] A. Shnirman et al. "Low- and High-Frequency Noise from Coherent Two-Level Systems". In: *Phys. Rev. Lett.* 94.127002 (2005).
- [3] J. Lisenfeld et al. "Measuring the temperature dependence of individual two-level systems by direct coherent control". In: *Phys. Rev. Lett.* 105.230504 (2010).
- [4] J. Lisenfeld et al. "Observation of directly interacting coherent two-level systems in an amorphous material". In: *Nat. Comm.* 6.6182 (2015).
- [5] Y. Shalibo et al. "Lifetime and Coherence of Two-Level Defects in a Josephson Junction". In: *Phys. Rev. Lett.* 105.177001 (2010).
- [6] J. Martinis et al. "Decoherence in Josephson Qubits from Dielectric Loss". In: *Phys. Rev. Lett.* 95.210503 (2005).
- [7] A. Romanenko et al. "Three-Dimensional Superconducting Resonators at $T < 20$ mK with Photon Lifetimes up to $\tau = 2$ s." In: *Phys. Rev. Appl.* 13.034032 (2020).
- [8] A. Bose et al. "Evolution of surface oxides and impurities in high vacuum heat treated Nb: A TEM and TOF-SIMS in-situ study, mechanism and repercussions on SRF cavity applications". In: *Appl. Surf. Sci.* 510.145464 (2020).